Published OnlineFirst September 29, 2009; DOI: 10.1158/0008-5472.CAN-09-1724

Design of Agonistic Altered Peptides for the Robust Induction of CTL Directed towards H-2D^b in Complex with the Melanoma-Associated Epitope gp100

Marianne J.B. van Stipdonk,[1] Daniel Badia-Martinez,[3] Marjolein Sluijter,[1] Rienk Offringa,[1] Thorbald van Hall,[2] and Adnane Achour[3]

Departments of [1]Immunohematology and Blood transfusion and [2]Clinical Oncology, Leiden University Medical Center, Leiden, the Netherlands; and [3]Center for Infectious Medicine, Department of Medicine, Karolinska University Hospital Huddinge, Karolinska Institutet, Stockholm, Sweden

Abstract

Immunogenicity of tumor-associated antigens (TAA) is often weak because many TAA are autoantigens for which the T-cell repertoire is sculpted by tolerance mechanisms. Substitutions at main anchor positions to increase the complementarity between the peptide and the MHC class I (MHC-I) binding cleft constitute a common procedure to improve binding capacity and immunogenicity of TAA. However, such alterations are tailored for each MHC-I allele and may recruit different CTL specificities through conformational changes in the targeted peptides. Comparative analysis of substituted melanoma-differentiation antigen gp100 in complex with H-2D^b revealed that combined introduction of glycine and proline residues at the nonanchor positions 2 and 3, respectively, resulted in an agonistic altered peptide with dramatically enhanced binding affinity, stability, and immunogenicity of this TAA. Peptide vaccination using the p2Gp3P-altered peptide version of gp100 induced high frequencies of melanoma-specific CTL in the endogenous CD8$^+$ repertoire. Crystal structure analysis of MHC/peptide complexes revealed that the conformation of the modified p2Gp3P-peptide was similar to the wild-type peptide, and indicated that this mimotope was stabilized through interactions between peptide residue p3P and the tyrosine residue Y159 that is conserved among most known MHC-I molecules throughout mammalian species. Our results may provide an alternative approach to enhance MHC stabilization capacity and immunogenicity of low-affinity peptides for induction of robust tumor-specific CTL. [Cancer Res 2009;69(19):7784–92]

Introduction

The identification of a large number of tumor-associated antigens (TAA) that may serve as targets for CD8$^+$ CTLs has stimulated research on the potential exploitation of MHC class I-binding peptide epitopes for immunotherapy of cancer (1, 2). An important category of TAA comprises nonmutated tissue differentiation antigens that represent overexpression or aberrant expression of the proteins (3). Due to immune tolerance, the avidity of anti-TAA T-cells is of moderate-to-low quality resulting in poor immunogenicity. Consequently, it is difficult to activate TAA-specific T cells upon using cognate low-affinity nonmodified tumor/self-peptide antigens. This represents a major challenge for the design of cancer vaccines.

Although clinical effectiveness has been disappointing until now (1), the use of peptides as therapeutics has received renewed enthusiasm due to recent advances in design, delivery, and stability of vaccine formulations (4, 5). The most common procedure to improve the effectiveness of vaccines comprising tumor/self-antigens is to increase the MHC binding affinity of TAA epitopes by substituting key peptide anchor positions with residues that display more appropriate properties (6–8). However, such tailor-based improvements may alter the conformation of the presented peptide and/or do not always result in enhanced T-cell recognition of the native target sequence (9, 10).

The melanocyte differentiation antigen gp100, an antigen naturally expressed by both normal melanocytes and the majority of malignant melanomas (11), is an attractive TAA candidate for use in vaccines. Previous studies showed that in contrast to the corresponding natural mouse peptide gp100$_{25\text{-}33}$ (EGSRNQDWL, hereafter called EGS), the human orthologue CTL epitope gp100$_{25\text{-}33}$ (KVPRNQDWL, KVP) induced "self"-reactive CTL responses (12). Although EGS and KVP differed only at the first three NH_2-terminal nonanchoring positions (p1-p3) and that both peptides contain the motif required for binding to H-2D^b, with an asparagine and a leucine residue at positions 5 (p5N) and 9 (p9L), respectively, KVP binds with a 100-fold higher affinity to H-2D^b. To elucidate the basis underlying this apparent paradox, as well as the relative contribution of the NH_2-terminal residues 1 to 3, functional and structural analyses of the two peptides and all permutated versions were performed.

In contrast to previous studies that aimed to optimize the complementarity between peptide anchoring residues and MHC pockets, our study shows that the combined introduction of a glycine and a proline at positions 2 (p2G) and 3 (p3P), respectively, enhanced binding affinity and stability of the modified peptides. The immunogenicity of the p2Gp3P-altered peptides was increased to a degree hitherto never observed, as measured through *in vitro* and *in vivo* assays. Vaccination with the modified peptide EGP (EGPRNQDWL) elicited high frequencies of EGS-specific CTL from the endogenous repertoire that efficiently targeted natural H-2D^b/EGS complexes on melanoma tumor cells.

Comparison of the crystal structures of H-2D^b in complex with EGS, KVP, and EGP revealed that the conformation of the three

Note: Supplementary data for this article are available at Cancer Research Online (http://cancerres.aacrjournals.org/).

M.J.B. van Stipdonk and D. Badia-Martinez contributed equally to this work.

T. van Hall and A. Achour are shared last authors.

Requests for reprints: Adnane Achour, Center for Infectious Medicine, Department of Medicine, F59, Karolinska University Hospital Huddinge, Karolinska Institutet, S-141 86, Stockholm, Sweden. Phone: 46-8-52486232; Fax: 46-8-30-42-76; E-mail: adnane.achour@ki.se and Thorbald van Hall, Department of Clinical Oncology, Leiden University Medical Center, 2333 ZA Leiden, the Netherlands. E-mail: T.van_Hall@LUMC.nl.

doi:10.1158/0008-5472.CAN-09-1724

Published OnlineFirst September 29, 2009; DOI: 10.1158/0008-5472.CAN-09-1724

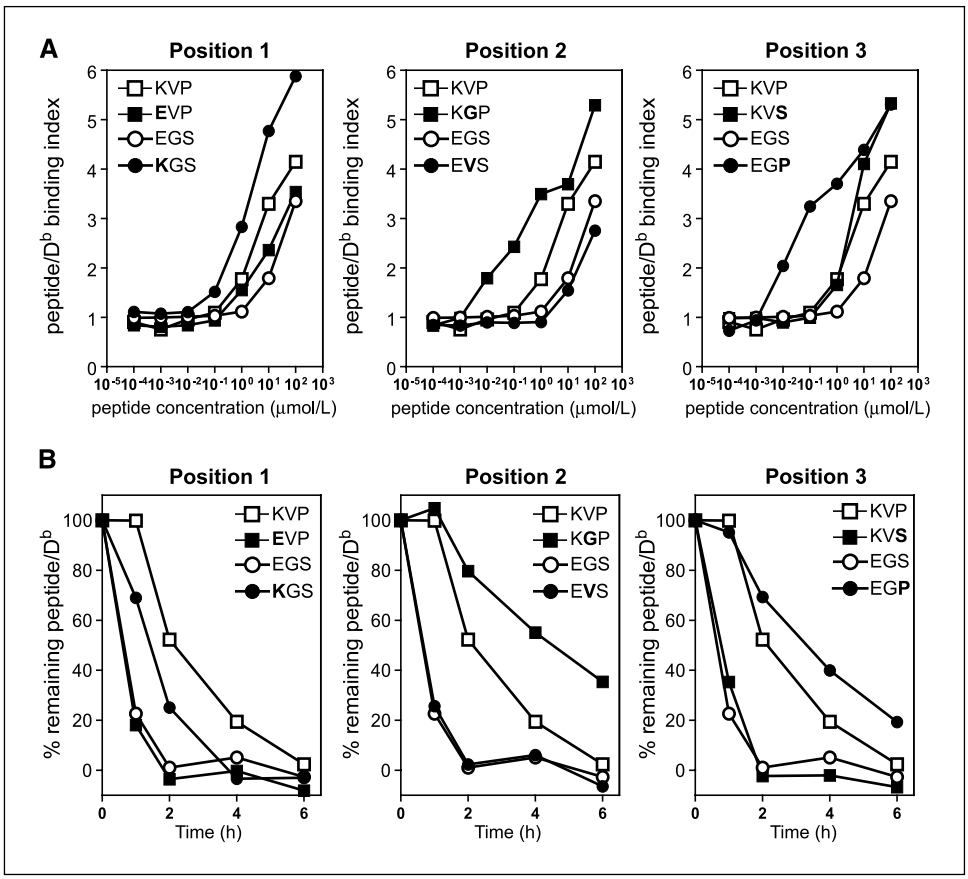

Figure 1. The combined p2Gp3P substitution results in higher binding affinity and improved stabilization of MHC-I expression. Peptide binding affinity (*top*) and MHC stabilizations assays (*bottom*) are shown. The effects of substitutions at peptide positions 1, 2, and 3 on binding affinity to H-2D^b (*A*) and on stability of H-2D^b complexes (*B*) are shown. All peptides are indicated by their first three NH_2-terminal residues. The substituted positions are in bold. Variants of EGS (*circles*) and KVP (*squares*) are shown. *A,* peptides KGS, KGP, and EGP bind with higher affinity to H-2D^b when compared with all other peptide variants as measured by MHC surface stabilization on RMA-S cells. Similar results were obtained in four separate experiments. *B,* peptides KGP and EGP display a superior capacity at stabilizing H-2D^b expression levels. Similar results were obtained in three separate experiments. Peptide/MHC binding affinity is expressed as index of MFI with peptide and without peptide. For the peptide/MHC stabilization assays, the MFI observed for each time point was calculated as a percentage of the MFI at t = 0 h.

peptides is similar. The p2Gp3P modifications in EGP establish novel essential interactions within the binding cleft of H-2D^b, mainly between p3P and heavy chain residue Y159, conserved among most known MHC-I sequences across species (13). In conclusion, this study suggests an alternative approach for the design of optimal peptide mimotopes that overcome self-tolerance and could be used as target antigens for immunotherapy of cancer.

Materials and Methods

Reagents. All gp100 peptide variants were used as 9-mers, unless indicated otherwise. Purity and integrity of all peptides was assessed with reversed phase high performance liquid chromatography and mass spectrometry. CpG oligodeoxynucleotide 1826 was synthesized in the Leiden Institute of Chemistry. Imiquimod was obtained as Aldara (5% imiquimod; 3M Health Care Ltd). In our hands, imiquimod has proven to be a stronger adjuvant than CpG. Thus, CpG was used for transgenic pmel expansion data presented in Fig. 2, whereas imiquimod was used for the expansion of endogenous T-cell populations in all other assays.

MHC binding affinity and stabilization assays. Peptide binding was assessed by cell surface stabilization of H-2D^b or H-2K^b on TAP-deficient RMA-S cells. Peptide/MHC binding affinity is expressed as index of mean fluorescence with peptide and without peptide. Peptides $E1A_{234-243}$ (SGPSNTPPEI; ref. 14) and MuLV $env_{189-196}$ (SSWDFITV; ref. 15) were used as optimal H-2D^b and H-2K^b binders, respectively. In peptide-dependent stabilization assays, TAP-deficient RMA-S cells were loaded with 10 μg/mL peptide for 1 h, washed, and incubated in AIM-V medium at 37°C. For stabilization assays, the mean fluorescence intensity (MFI) observed for each time point was calculated as a percentage of the MFI at t = 0 h. Surface expression of H-2D^b and H-2K^b was measured by flow cytometry using FITC-conjugated monoclonal antibody KH95 and 28.14.8S (H-2D^b) and B8.24.3 (H-2K^b), respectively (BD Pharmingen/BD Biosciences).

Mice. Male C57BL/6 mice were purchased from Iffa Credo. TCR transgenic mice containing $gp100_{25-33}$/H-2D^b-specific T-cell receptors (designated as pmel) were a gift from Dr. N.P. Restifo (National Cancer Institute, Bethesda, Maryland) and bred to express the congenic marker CD90.1. All mice were housed under specific pathogen-free conditions and used at 6 to 12 wk of age. Experiments were performed in accordance with Dutch national legislation and institutional guidelines.

Immunogenicity in TCR-transgenic pmel cells. Lymphocytes from spleen and lymph nodes of naïve CD90.1-positive pmel mice were isolated and enriched for T lymphocytes by nylon wool. Pmel cells were labeled with 5 μmol/L carboxyfluorescein diacetate succinimidyl ester (CFSE; Molecular Probes) and 3×10^6 CD8$^+$ T lymphocytes were adoptively transferred by injection into the tail vein. Mice were immunized 1 d later through s.c. injection of 50 μg $gp100_{25-33}$ mixed in PBS with 25 μg CpG. After 4 d, single-cell suspensions from spleen, draining, and nondraining lymph nodes were prepared for analysis. Lymphocytes were incubated for 3 h with 1 μg/mL EGS and GolgiPlug (BD bioscience) and stained thereafter with fluorochrome-labeled antibodies for intracellular IFN-γ (XMG1.2) in combination with CD8α (53-6.7) and CD90.1 (HIS51; BD biosciences). Cells were analyzed using a FACS Calibur flow cytometer and Cell Quest Pro software (BD biosciences).

***In vivo* analysis of endogenous T-cell repertoire.** For priming of endogenous T cells, C57BL/6 mice were shaved on the flank and injected s.c. at days 0 and 7 with PBS alone or 50 to 150 μg 20-mer long peptides (EGS-long: AVGAL*EGS*RNQDWLGVPRQL, KVP-long: AVGAL*KVP*RNQDWLGVPRQL, or EGP-long: AVGAL*EGP*RNQDWLGVPRQL) in PBS. Immediately following injection, 60 mg of 5% imiquimod cream (Aldara) were applied to the skin at the injection site. Where indicated, mice received an additional i.p. injection of 600,000 IU human interleukin 2 (IL-2; Novartis) on the day of the second vaccination and one on the day thereafter. On day 10 to 15, splenocytes were harvested and stimulated *in vitro* with

Published OnlineFirst September 29, 2009; DOI: 10.1158/0008-5472.CAN-09-1724

lipopolysaccharide-matured, irradiated (3,000 rad) dendritic cells (D1; ref. 16) loaded with 5 μg/mL peptide. After 6 d, viable cells were isolated by ficoll density gradient and were either directly stained with a CD8-specific antibody and H-2D^b/EGS tetramers (a gift from Dr. Schumacher, the Netherlands Cancer Institute, Amsterdam) or stained with antibodies specific for CD8 and intracellular IFN-γ following overnight incubation with 5 μg/mL EGS peptide. All analyses were performed using flow cytometry. Cytolytic activity of the peptide-stimulated splenocyte cultures

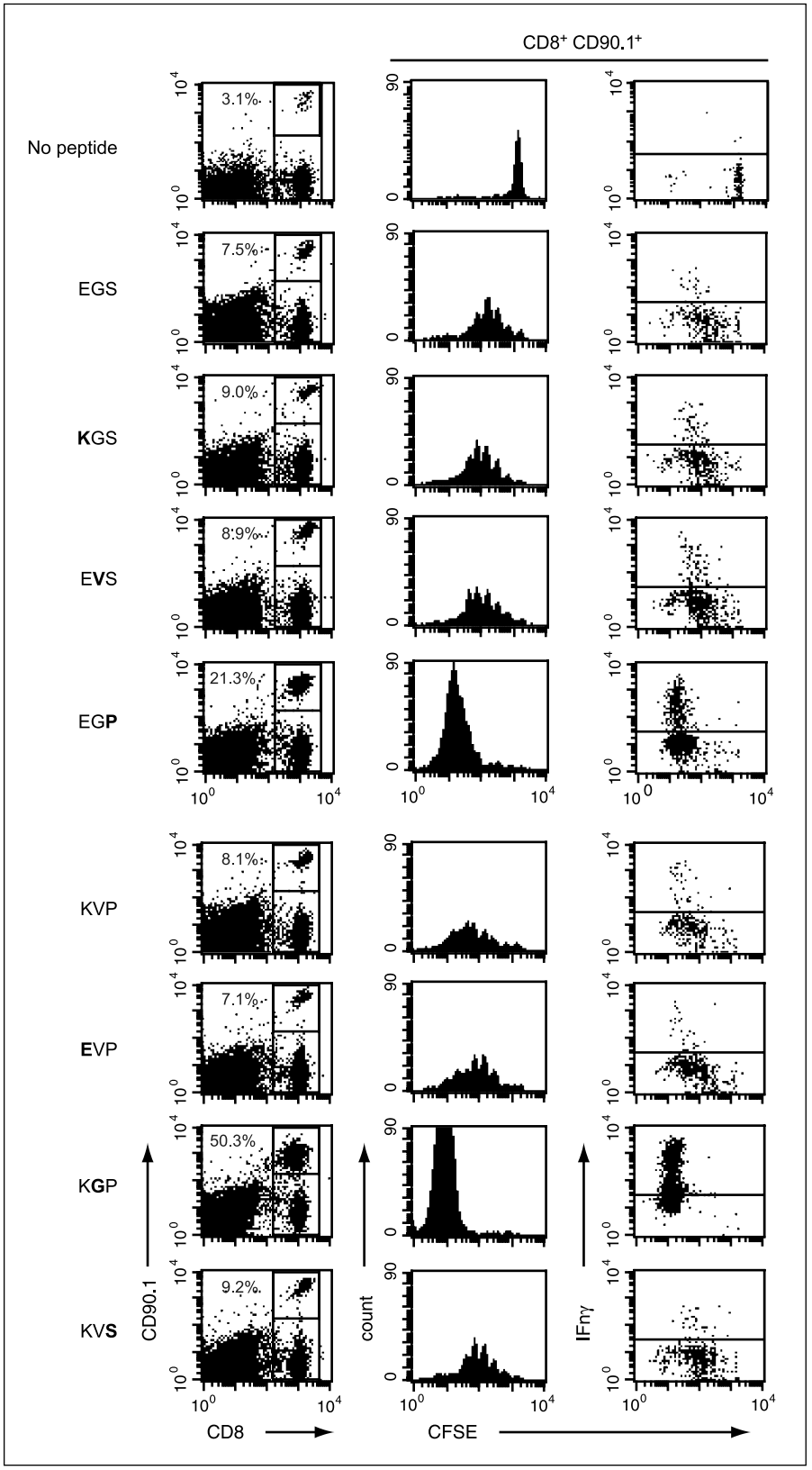

Figure 2. KGP and EGP are very immunogenic in a TCR-transgenic model system. The immunogenicity of all peptide variants was tested *in vivo* using C57BL/6 mice that received CFSE-labeled CD90.1$^+$ pmel T-cells. Mice were immunized s.c. with indicated peptides mixed with CpG. After 4 d, harvested lymph node cells were stimulated for 3 h with 1 μg/mL EGS. Cells were stained for CD8, CD90.1, and IFN-γ. Size of pmel population (CD8$^+$CD90.1$^+$ of total CD8$^+$ pool), degree of cell division (mean CFSE fluorescence of pmel), and percentage of IFN-γ$^+$ producing effector cells (IFN-γ$^+$ of pmel) were analyzed by flow cytometry. Mutated positions are in bold.

Published OnlineFirst September 29, 2009; DOI: 10.1158/0008-5472.CAN-09-1724

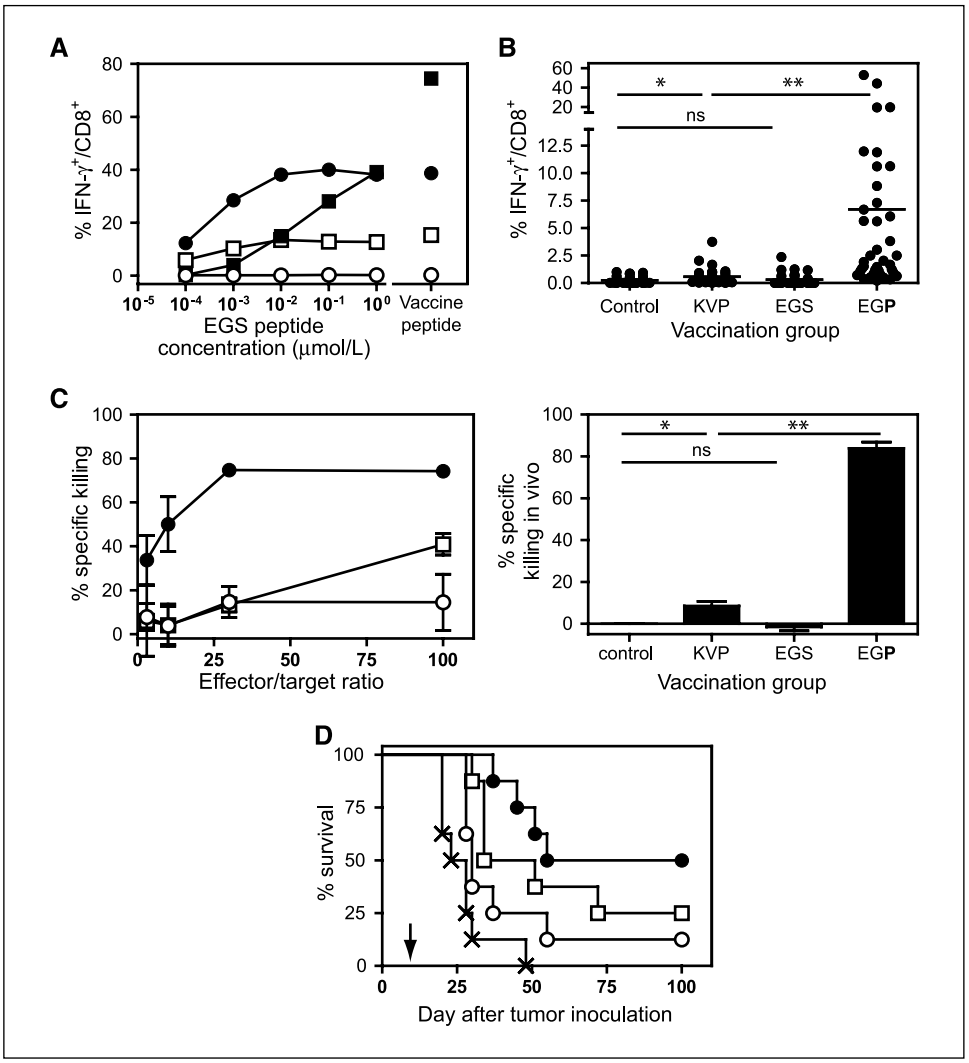

Figure 3. Immunization with EGP efficiently elicited endogenous antitumor CD8$^+$ T-cell responses. *A,* C57BL/6 mice were immunized with KVP (□), KGP (■), EGS (○), or EGP (●). After 10 d, harvested spleen cells were stimulated once with respective peptides *in vitro* and tested against the immunizing vaccine peptide and titrated concentrations of EGS. IFN-γ production was measured intracellularly by flow cytometry and quantified as percentage positive cells of CD8$^+$ T cells. One representative experiment out of three is displayed (three mice per group). *B,* frequencies of EGS-specific CD8$^+$ T cells were directly monitored from the blood of immunized C57BL/6 mice. Immunizations were performed with 20-mer long peptides comprising KVP, EGS, or EGP sequences and topical imiquimod as adjuvants (38 mice per group). *, $P \leq 0.05$; **, $P < 0.001$, and Student's *t* tests were performed using GraphPad software. *C, left,* spleens and lymph nodes harvested from peptide-immunized mice from *B* were stimulated once *in vitro* with the same peptide KVP (□), EGS (○), and EGP (●), and killing capacity was tested in a DNA fragmentation assay against B16 melanoma cells. *C, right, in vivo* killing assay in which C57BL/6 mice were injected with equal numbers of two differentially CFSE-labeled target cells. CFSE low- and high-labeled targets were exogenously pulsed with EGS and a control peptide, respectively. Percentage of killing was calculated by the ratio of the two targets in spleens of mice. Groups of four mice were analyzed. *Columns,* mean results; *bars,* SEM. *, $P \leq 0.05$; **, $P < 0.001$, and Student's *t* tests were performed using GraphPad software. *D,* B16 tumor cells were injected s.c. into naïve C57BL/6 mice. After 8 d, mice were vaccinated once with peptides KVP (□), EGS (○), and EGP (●) or naïve (×) in combination with nonstimulated pmel cells. Mice were sacrificed when tumor sizes exceeded above 1 cm^3. Kaplan-Meier survival curves of EGP-treated group ($n = 9$) and controls were significantly different (log-rank test in GraphPad); $P = 0.0007$. *Arrow,* the start of treatment (day 9). Comparable results were obtained in an additional independent experiment.

was determined using tritium-thymidine–labeled B16 melanoma cells in a DNA fragmentation assay (17). Peripheral blood lymphocytes samples were collected on day 13, and IFN-γ production following overnight stimulation with EGS was determined. Plots are gated on live CD8$^+$ lymphocytes.

***In vivo* cytotoxicity of endogenous gp100-specific CTL.** C57BL/6 mice were vaccinated with 20-mer long peptides and imiquimod as described above. The mice were injected 8 d later i.v. with a mix of nonameric peptide-pulsed CFSE-labeled splenocytes as described previously (18). Briefly, spleens from CD90.1 congenic C57BL/6 mice were passed through nylon wool. Half of the splenocytes was pulsed with EGS and labeled with 0.5 μmol/L CFSE, whereas the other half was pulsed with control peptide $E1A_{234\text{-}243}$ and labeled with 5 μmol/L CFSE. Target cell populations were washed, mixed, and 50×10^6 cells were injected per recipient mouse. Spleens of immunized mice were harvested after 2 d, stained with CD3-, CD8-, and CD90.1-specific antibodies, and analyzed with flow cytometry. Percentage killing was calculated as the ratio between the numbers of EGS-pulsed targets and control-pulsed targets.

Tumor protection experiments. C57BL/6 mice were inoculated with 20,000 B16F10 tumor cells s.c. in the flank. After 8 d, mice were adoptively transferred with 10^6 naïve pmel cells in the tail vein. Next day and 1 wk later, mice were shaved on the contralateral flank and injected s.c. with PBS alone or 150 μg murine $gp100_{20\text{-}39}$ long peptide containing either EGS, EGP, or KVP. Immediately following injection, 60 mg Aldara cream were applied to the skin at the injection site. Mice were also injected i.p. with 600,000 IU human IL-2 on the day of the second vaccination and on the day thereafter.

Published OnlineFirst September 29, 2009; DOI: 10.1158/0008-5472.CAN-09-1724

Tumor growth was measured in three dimensions twice weekly. Mice were sacrificed when tumors exceeded 1 cm^3.

Data collection and processing. Refolding and purification of H-2D^b in complex with EGS, KVP, and EGP were conducted as previously described (19). Crystals were obtained in hanging drops by vapor diffusion in 1.8M ammonium sulfate and 0.1M TrisCl (pH 9.0) at 4°C. Crystals were cryoprotected using 20% glycerol and diffraction data were processed using XDS (20).

Structure determination and refinement. All structures were solved by molecular replacement using PHASER (21) with H-2D^b/gp33 (19) as a search model. Model building was performed with COOT (22) combined with refinement using REFMAC (23). TLS refinement was introduced in the

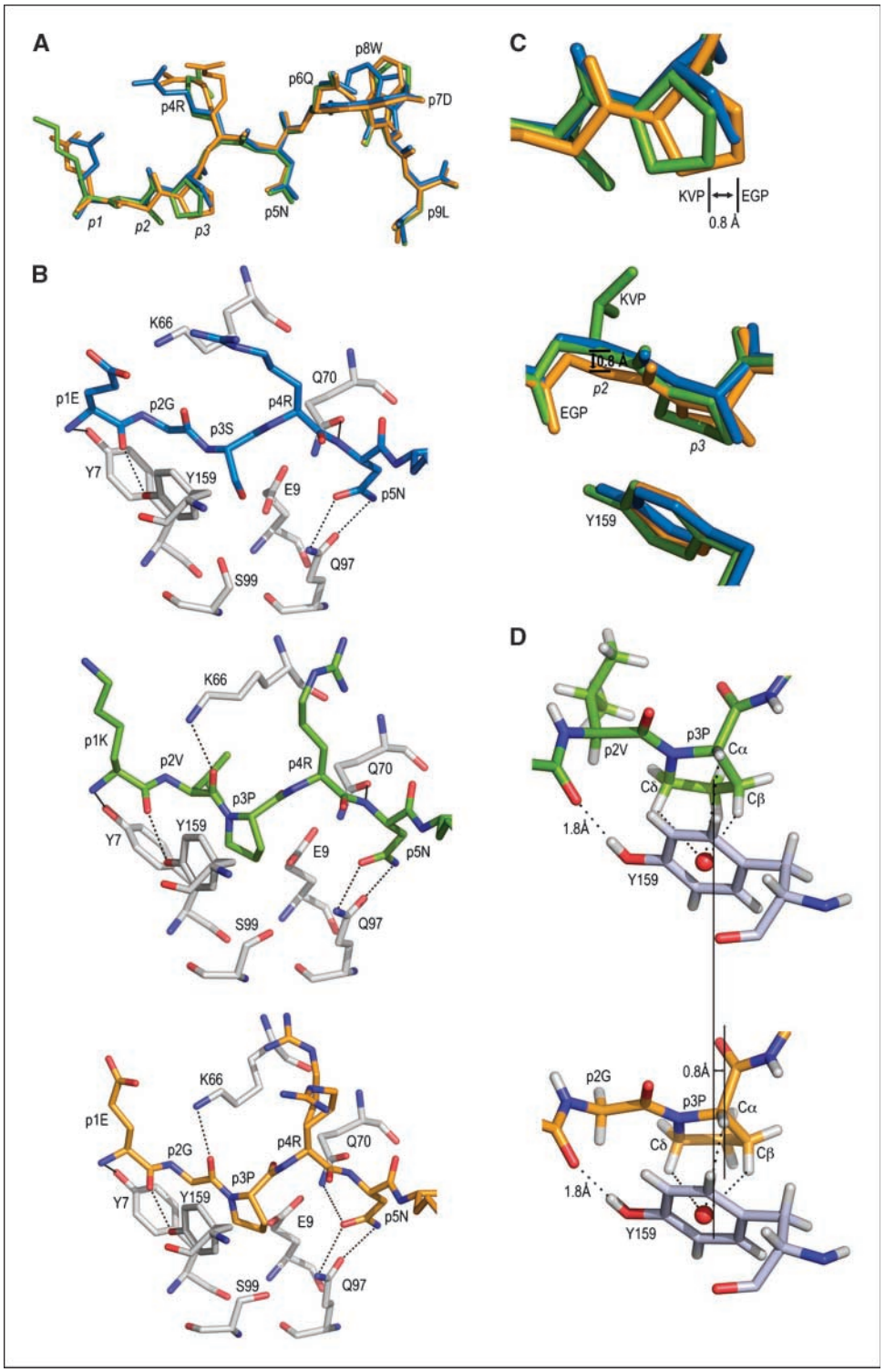

Figure 4. Structural basis underlying enhanced binding capacity and immunogenicity. *A,* the conformation of EGS (*blue*), KVP (*green*), and EGP (*orange*) is similar. *B,* detailed description of the structural interactions between residues from the C-pocket of H-2D^b and EGS (*top*), KVP (*middle*), or EGP (*bottom*). Carbon atoms for EGS (*blue*), KVP (*green*), EGP (*orange*), and H-2D^b (*white*) residues are shown. *Red,* oxygens; *blue,* nitrogens. *Dotted lines,* hydrogen bond interactions. *C,* introduction of p2G in EGP results in a lateral shift at the p2 Cα atom of 0.8Å (*top*), resulting in further translation by 0.8Å at the Cγ atom of p3P along the length of the peptide (*bottom*) and in enhanced geometry between the side chains of p3P and Y159. Residues belonging to the H-2D^b/EGS (*blue*), H-2D^b/KVP (*green*), and H-2D^b/EGP complexes (*orange*) shown. *D,* detailed description of the structural interaction between p3P and Y159 in H-2D^b/KVP and H-2D^b/EGP. Substitution of a glycine residue in EGP instead of a valine in KVP allows for a small translational movement of the side chain of p3P that results in enhanced geometry with the side chain of Y159. The carbon backbones for KVP (*green*), EGP (*orange*), and H-2D^b (*white*) residues shown. *Red,* oxygen; *blue,* nitrogen and *white,* modelized hydrogen atoms. The center of symmetry of the ring of Y159 is indicated with a red ball and the pyrrolidine CH-groups that form CH-π interactions with Y159 are indicated. *Vertical line,* the observed shift of p3P between KVP and EGP.

Published OnlineFirst September 29, 2009; DOI: 10.1158/0008-5472.CAN-09-1724

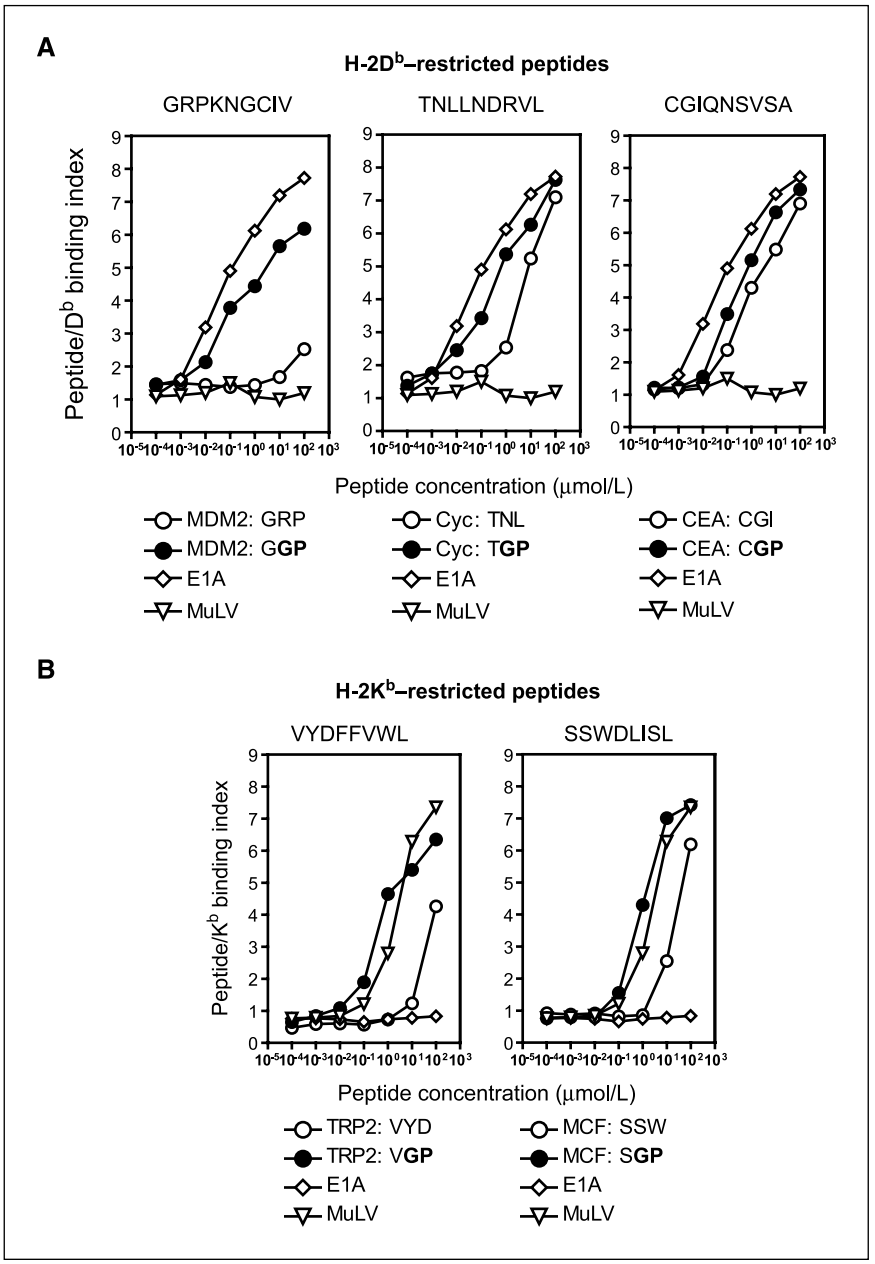

Figure 5. Introduction of the p2Gp3P combination in H-2D^b– and H-2K^b–restricted endogenous TAA peptides enhances binding affinity. Introduction of p2Gp3P in the weakly binding H-2D^b–restricted peptides MDM2 ($P = 0.002$; *A*), cyclin D1 ($P < 0.0001$; *A*) as well as in the H-2K^b restricted peptides TRP2 ($P = 0.003$; *B*) and MCF ($P = 0.01$; *B*) enhanced significantly their binding affinity. Although the introduction of p2Gp3P substitutions in the peptide CEA with intermediary affinity to H-2D^b increased binding affinity marginally ($P = 0.122$; *A*), the same result was consistently observed in each performed experiment. Wild-type (○) and p2Gp3P-substituted peptides (●) are shown. Peptides E1A (◇) and MuLV (Δ) were used as positive controls for binding to H-2D^b and H-2K^b, respectively. Peptide binding assays were repeated thrice.

last stages of refinement. Data collection and refinement statistics are summarized in Supplementary Table S1.

Results and Discussion

Combined p2Gp3P substitution increases binding affinity and MHC-I stabilization capacity of altered peptides. To establish the relative contribution of peptide residues p1 to p3 to the observed higher binding affinity of KVP to H-2D^b, six nonameric peptide variants corresponding to single amino acid permutations between EGS and KVP were generated. The binding affinity of peptides was determined through cell surface expression of H-2D^b on TAP-deficient RMA-S cells (Fig. 1*A*). Since it has been previously shown that stabilization of MHC-I by modified peptides enhances immunogenicity (24, 25), the capacity of all peptides to stabilize cell surface expression of H-2D^b was also assessed (Fig. 1*B*).

Introduction of a lysine at position 1 of gp100 improves both its binding affinity and the stability of the complex as indicated upon comparing KGS and KVP with EGS and EVP, respectively (Fig. 1). This is well in line with previous studies in which substitution of a lysine at position 1 altered the binding affinity of modified peptides to H-2D^b (26) or H-2K^b (27, 28). Although the substitution of glycine to valine at position 2 (pG2V) did not modify the poor binding affinity and complex stability of EGS and EVS, the converse substitution (pV2G) improved both binding affinity and complex stabilization of KGP when compared with KVP (Fig. 1). Thus, surprisingly, the removal of the side chain of the valine residue from the B-pocket upon mutating p2V to a glycine, in combination with a proline residue at position 3 of the peptide, was favorable for both binding affinity and stabilization capacity. Accordingly, substitution of serine in EGS to a proline also resulted in a striking improvement of binding

Published OnlineFirst September 29, 2009; DOI: 10.1158/0008-5472.CAN-09-1724

affinity (of at least a 100-fold) and MHC stabilization capacity (Fig. 1).

Taken together, our results show that the p2Gp3P combination dramatically improved the binding affinity and the MHC stabilization capacity of KGP and EGP. Mutation of a valine in KVP to a glycine in KGP increased both binding affinity and stabilization of H-2D^b (Fig. 1), implying that the effect of a proline residue at p3 was improved by the introduction of a glycine in the flanking residue p2. Similarly, introduction of a proline at position 3 in EGP dramatically improved both affinity and stability when compared with EGS (Fig. 1). The interdependency of the two residues is shown upon direct comparison of peptides harboring p2Vp3P or p2Gp3P (Supplementary Fig. S1). Our results indicate that (*a*) the potential effects of a modification at a specific position of the altered peptide onto adjacent peptide residues should be carefully evaluated and (*b*) modification of the size of a residue to increase interactions with MHC pockets can be directly detrimental to the overall binding affinity of the altered peptides.

The p2Gp3P-substituted peptides are highly immunogenic *in vivo*. The peptides EGS, KVP, and the six altered analogues were tested using T-cell receptor transgenic pmel cells, specific for H-2D^b in complex with EGS (29). CFSE-labeled CD8$^+$ pmel T-cells were adoptively transferred into CD90.2 congenic host mice that were subsequently vaccinated with the eight different peptide variants. The pmel T-cell responses were assessed in terms of expansion, number of divisions, and IFN-γ production in draining lymph nodes (Supplementary Fig. S2; Fig. 2). Immunization with EGS resulted in limited proliferation and activation of pmel cells, whereas nonimmunized mice did not harbor any proliferated CTL. In contrast, immunization with EGP resulted in significant clonal expansion and IFN-γ production of pmel T cells. As expected, immunization with KVP resulted in slightly higher proliferation when compared with EGS (Fig. 2). However, IFN-γ production and cell division were limited. Again, immunization with KGP resulted in dramatic increases of pmel activation (Supplementary Fig. S1*B–D*; Fig. 2). Importantly, similar results were also obtained in spleen and nondraining lymph nodes, indicating that the activated pmel cells harbored the capacity to spread systemically (Supplementary Fig. S3). In conclusion, the introduced p2Gp3P modifications in EGP and KGP result in strong *in vivo* immunogenicity combined with increased binding affinity and strong stabilization of H-2D^b, generating a very potent peptide vaccine.

Vaccination with EGP induces robust CTL responses from the endogenous T-cell repertoire. Groups of C57BL/6 mice were vaccinated with each of EGS, KVP, and the p2Gp3P-altered peptides EGP and KGP in combination with the TLR7 ligand imiquimod as an adjuvant (30). The reactivity of vaccine-induced CD8$^+$ T cells isolated from spleens and lymph nodes was analyzed *in vitro* (Fig. 3*A*). Vaccination and *in vitro* stimulation with EGS did not yield any detectable peptide-specific T-cells, whereas vaccination and stimulation with KVP led to significant numbers of KVP-reactive T cells that efficiently cross-reacted with EGS. Interestingly, KGP was strikingly immunogenic in C57BL/6 mice and up to 75% of all endogenous CD8$^+$ T cells in *ex vivo* cultures were specific for this peptide. However, KGP-reactive T cells cross-reacted with EGS only at relatively high concentrations, indicating that KGP promoted the expansion of T cells with a different fine specificity. Finally, EGP-induced T-cell responses displayed the most favorable characteristics: they were present at high frequencies and cross-reacted to very low concentrations of the natural target EGS. Thus, in contrast to KGP, residue p1E in EGP most likely constrains the recruited T-cell pool to cells that cross-react with EGS. Due to the relatively lower cross-reactivity displayed by KGP-induced T cells toward the original peptide EGS, we hereafter focused our analyses on EGP.

Vaccination with EGP induces melanoma-reactive CTL. Peptide vaccination can be strongly improved through the use of longer peptides that comprise minimal CTL epitopes in combination with adequate adjuvants that activate the innate immune system (4, 18). The immunotherapeutic potential of EGP was assessed against the aggressive B16 melanoma that expresses the gp100 antigen EGS. *Ex vivo* analyses of C57BL/6 mice immunized with EGS-long (AVGAL*EGS*RNQDWLGVPRQL), KVP-long (AVGAL-*KVP*RNQDWLGVPRQL), or EGP-long (AVGAL*EGP*RNQDWLGVP-RQL) combined with topical application of imiquimod resulted in very high frequencies of EGS-specific CD8$^+$ T cells in the blood of EGP-injected animals, with numbers up to 50% of the total CD8$^+$ cell population (Fig. 3*B*), clearly overruling the potency of the other peptides. Further analysis with tetramers of H-2D^b/EGS complexes corroborated these results (Supplementary Fig. S4). The CD8$^+$ T cells raised by EGP efficiently killed B16 melanoma cells *in vitro* (Fig. 3*C, left*) as well as peptide-loaded targets *in vivo* (Fig. 3*C, right*). In all experiments, KVP performed better than EGS, but was far less efficient when compared with EGP. In all animals immunized with EGP, the induced CTL population displayed a broad repertoire of TCR variable regions comparable with other peptide variants (Supplementary Fig. S5). The relatively higher frequency of Vβ13$^+$ TCRs in all four tested peptides indicates that this segment optimally suites the MHC/peptide complex. Of note, Vβ13 is also used by the transgenic pmel TCR. Finally, the immunotherapeutic potential of EGP was tested against established B16 mouse melanomas. C57BL/6 mice were inoculated with a tumorigenic dose of melanoma and treated from day 9, when subclinical tumors were established. Therapeutic vaccination with EGP-long led to significant numbers of CTLs in blood and within tumor beds, resulting in a delay of tumor outgrowth by 11 days (data not shown). Addition of naïve pmel cells at day 8 in the treatment scheme was sufficient to eradicate established melanomas in half of the EGP-treated group (Fig. 3*D*). Interestingly, no overt sign of autoimmune pathology or ocular autoimmunity (31) was observed in the surviving mice during the time frame of the experiments (4 months). In conclusion, the introduction of a proline residue at position 3 in the very weak tumor CTL epitope EGS transformed it into the strongly agonistic peptide EGP that can be used as a powerful vaccine capable of inducing effective antitumor CTL responses.

Structural basis underlying improved binding stability and immunogenicity in p2Gp3P-altered peptides. The overall conformation of the peptide-binding clefts is conserved in the crystal structures of H-2D^b in complex with EGS, KVP, and EGP, with overall root mean square deviations inferior to 1.1Å for C_α atoms of residues 1-176. Importantly, the conformation of all residues that potentially interact with the TCR and the two main anchor positions p5N and p9L is conserved among all three MHC complexes (Supplementary Fig. S6; Fig. 4*A*) and can thus not explain the differences in binding affinity and stabilization. Furthermore, similar amounts of hydrogen bond interactions are formed between H-2D^b and the three peptides.

However, comparative structural analysis indicated subtle but important differences at positions 2 and 3 as a structural basis for the higher affinity and stability of EGP when compared with KVP and EGS. A hydrogen bond interaction is formed in all three structures between the hydroxyl group of Y159, conserved among

most known MHC-I molecules (13), and the oxygen atom of peptide residue p1, resulting in a precise orientation of the side chain of Y159 (Fig. 4*B*). Proteins can use the hydroxyl of tyrosines to position their ring precisely (32). Furthermore, the involvement of the hydroxyl group of a tyrosine as a hydrogen bond donor enhances the electronegativity of the tyrosine ring and promotes the formation of CH-π interactions with adjacent residues, such as in this case p3P in the bound peptide (32, 33).

Although few interactions are formed between H-2D^b and residues p2G and p3S in H-2D^b/EGS (Fig. 4*B*), the side chain of p2V in H-2D^b/KVP makes van der Waals contacts with residues Y7 and Y45 in the B-pocket. Importantly, the pyrrolidine ring of p3P fits better within the C pocket, when compared with p3S in H-2D^b/EGS, mostly through extensive interactions with residue Y159. CH-π interactions are formed between p3P and Y159. Engagement of the pyrrolidine ring of a proline with an aromatic ring, especially when it leads to CH-π interactions, provides substantial binding energy (32–36). Indeed, CH-π interactions play an important role for molecular recognition in biological receptors and contribute significantly to the overall stability of proteins (34, 37).

Our functional studies pointed at the strong interdependence between p2G and p3P in the p2Gp3P-altered peptides. The bulky pyrrolidine ring of the proline restricts the conformational freedom of the preceding residue (38), and although p2V is not unfavorable to binding of KVP, the positioning of the side chain of p2V will be constrained by sterical hindrances within the in the acidic B-pocket. The parallel positioning of the side chains of prolines and tyrosines is important for optimal formation of CH-π interactions (32–34). Thus, as a consequence of the positioning of p2V within the B-pocket, CH-π interactions between p3P and Y159 are not optimal in H-2D^b/KVP. In contrast, the p2Gp3P combination in H-2D^b/EGP allows for a translational movement of this section of the peptide (Fig. 4*C*) with at least three consequences. First, the side chain of p3P is shifted by 0.8Å in H-2D^b/EGP when compared with H-2D^b/KVP, resulting in an optimal positioning of p3P and Y159 (Fig. 4*D*). As a consequence, van der Waals, CH-π, and electrostatic interactions are enhanced. Second, the side chain of p3P binds deeper within the peptide binding cleft (0.8Å shift when compared with p3P in H-2D^b/KVP), increasing the van der Waals interactions with H-2D^b residues E9, Q97, S99, and Y159. Third, CH-O interactions are formed between the C_δ-H group of p3P and residues E9 and S99 (0.8Å shift when compared with p3P in H-2D^b/KVP). In conclusion, the p2Gp3P combination allows for optimal CH-π and van der Waals interactions between p3P and heavy chain residue Y159, conserved among most known MHC-I molecules (13).

Insertion of p2Gp3P in several cancer-associated peptides enhances their binding affinity to H-2D^b and H-2K^b. To assess the potential broadness of the applicability of our discovery, the binding affinity of a panel of p2Gp3P-substituted peptides was tested in H-2D^b and H-2K^b. Introduction of p2Gp3P in the low-affinity H-2D^b–restricted TAA MDM2$_{441\text{-}449}$ (39), cyclin D1$_{20\text{-}28}$ (39) and the H-2K^b-binding TRP2$_{181\text{-}188}$ (40), and MCF env$_{143\text{-}150}$ (15) led to significant increase of binding affinity (Fig. 5), suggesting that our approach may be applicable to a broad range of weakly binding peptides restricted to H-2D^b and H-2K^b. Although the introduction of p2Gp3P substitutions in the peptide carcinoembryonic antigen (CEA; ref. 41) with intermediary affinity to H-2D^b increased binding affinity marginally, this result was obtained in three separate experiments. Due to the conservation of the heavy chain residue Y159 among most known MHC class I alleles, one may speculate that similar results could be obtained with weakly binding peptides restricted to other mouse and human MHC alleles.

Concluding remarks. This study shows that the p2Gp3P-altered peptide EGP mimics the wild-type melanoma-associated EGS, enhancing the stabilization of MHC complexes and immunogenicity (42). Structural conservation relieves concerns on unwanted side effects, such as the generation of CTL populations that do not properly cross-react with the natural ligand, as recently reported for MART-1/MelanA (10).

Disclosure of Potential Conflicts of Interest

The authors declare no conflict of interest.

Acknowledgments

Received 5/13/09; revised 7/22/09; accepted 8/6/09; published OnlineFirst 9/29/09.

Grant support: Netherlands Organisation for Scientific Research, the Macropa and Gratama foundations (M.J.B. van Stipdonk), the Swedish Medical Research Council, the Swedish Cancer Society, the Swedish Childhood Cancer Foundation, and the Swedish National Board of Health and Welfare (A. Achour).

The costs of publication of this article were defrayed in part by the payment of page charges. This article must therefore be hereby marked *advertisement* in accordance with 18 U.S.C. Section 1734 solely to indicate this fact.

We thank ESRF-France, BESSY-Germany, and MAX-Sweden for allowing us access to synchrotron beamlines.

References

1. Rosenberg SA, Yang JC, Restifo NP. Cancer immunotherapy: moving beyond current vaccines. Nat Med 2004;10:909–15.
2. Van Der Bruggen P, Zhang Y, Chaux P, et al. Tumor-specific shared antigenic peptides recognized by human T cells. Immunol Rev 2002;188:51–64.
3. Boon T, Coulie PG, Van den Eynde BJ, van der Bruggen P. Human T cell responses against melanoma. Annu Rev Immunol 2006;24:175–208.
4. Melief CJ, van der Burg SH. Immunotherapy of established (pre)malignant disease by synthetic long peptide vaccines. Nat Rev Cancer 2008;8:351–60.
5. Purcell AW, McCluskey J, Rossjohn J. More than one reason to rethink the use of peptides in vaccine design. Nat Rev Drug Discov 2007;6:404–14.
6. Borbulevych OY, Baxter TK, Yu Z, Restifo NP, Baker BM. Increased immunogenicity of an anchor-modified tumor-associated antigen is due to the enhanced stability of the peptide/MHC complex: implications for vaccine design. J Immunol 2005;174:4812–20.
7. Chen JL, Stewart-Jones G, Bossi G, et al. Structural and kinetic basis for heightened immunogenicity of T cell vaccines. J Exp Med 2005;201:1243–55.
8. Webb AI, Dunstone MA, Chen W, et al. Functional and structural characteristics of NY-ESO-1-related HLA A2-restricted epitopes and the design of a novel immunogenic analogue. J Biol Chem 2004;279:23438–46.
9. Denkberg G, Klechevsky E, Reiter Y. Modification of a tumor-derived peptide at an HLA-A2 anchor residue can alter the conformation of the MHC-peptide complex: probing with TCR-like recombinant antibodies. J Immunol 2002;169:4399–407.
10. Speiser DE, Baumgaertner P, Voelter V, et al. Unmodified self antigen triggers human CD8 T cells with stronger tumor reactivity than altered antigen. Proc Natl Acad Sci U S A 2008;105:3849–54.
11. Kawakami Y, Eliyahu S, Jennings C, et al. Recognition of multiple epitopes in the human melanoma antigen gp100 by tumor-infiltrating T lymphocytes associated with *in vivo* tumor regression. J Immunol 1995;154:3961–8.
12. Overwijk WW, Tsung A, Irvine KR, et al. gp100/pmel 17 is a murine tumor rejection antigen: induction of "self"-reactive, tumoricidal T cells using high-affinity, altered peptide ligand. J Exp Med 1998;188:277–86.
13. Watts S, Wheeler C, Morse R, Goodenow RS. Amino acid comparison of the class I antigens of mouse major histocompatibility complex. Immunogenetics 1989;30:390–2.
14. Feltkamp MC, Vierboom MP, Kast WM, Melief CJ. Efficient MHC class I-peptide binding is required but does not ensure MHC class I-restricted immunogenicity. Mol Immunol 1994;31:1391–401.
15. Sijts AJ, De Bruijn ML, Ressing ME, et al. Identification of an H-2 Kb-presented Moloney murine leukemia virus cytotoxic T-lymphocyte epitope that displays enhanced recognition in H-2 Db mutant bm13 mice. J Virol 1994;68:6038–46.

Published OnlineFirst September 29, 2009; DOI: 10.1158/0008-5472.CAN-09-1724

16. Winzler C, Rovere P, Rescigno M, et al. Maturation stages of mouse dendritic cells in growth factor-dependent long-term cultures. J Exp Med 1997;185: 317–28.

17. Matzinger P. The JAM test. A simple assay for DNA fragmentation and cell death. J Immunol Methods 1991; 145:185–92.

18. Bijker MS, van den Eeden SJ, Franken KL, Melief CJ, Offringa R, van der Burg SH. CD8+ CTL priming by exact peptide epitopes in incomplete Freund's adjuvant induces a vanishing CTL response, whereas long peptides induce sustained CTL reactivity. J Immunol 2007;179:5033–40.

19. Achour A, Michaelsson J, Harris RA, et al. A structural basis for LCMV immune evasion: subversion of H-2D(b) and H-2K(b) presentation of gp33 revealed by comparative crystal structure Analyses. Immunity 2002;17:757–68.

20. Kabsch W. Automatic processing of rotation diffraction data from crystals of initially unknown symmetry and cell constants. J Appl Cryst 1993;26:795–800.

21. McCoy AJ. Solving structures of protein complexes by molecular replacement with Phaser. Acta Crystallogr D Biol Crystallogr 2007;63:32–41.

22. Emsley P, Cowtan K. Coot: model-building tools for molecular graphics. Acta Crystallogr D Biol Crystallogr 2004;60:2126–32.

23. Murshudov GN, Vagin AA, Dodson EJ. Refinement of macromolecular structures by the maximum-likelihood method. Acta Crystallogr D Biol Crystallogr 1997;53:240–55.

24. Sette A, Vitiello A, Reherman B, et al. The relationship between class I binding affinity and immunogenicity of potential cytotoxic T cell epitopes. J Immunol 1994;153:5586–92.

25. van der Burg SH, Visseren MJ, Brandt RM, Kast WM, Melief CJ. Immunogenicity of peptides bound to MHC class I molecules depends on the MHC-peptide complex stability. J Immunol 1996;156:3308–14.

26. Wang B, Sharma A, Maile R, Saad M, Collins EJ, Frelinger JA. Peptidic termini play a significant role in TCR recognition. J Immunol 2002;169:3137–45.

27. Chen W, Fecondo J, McCluskey J. The structural influence of individual residues located within peptide antigen depends upon their sequence context. Mol Immunol 1994;31:1069–75.

28. Chen W, Khilko S, Fecondo J, Margulies DH, McCluskey J. Determinant selection of major histocompatibility complex class I-restricted antigenic peptides is explained by class I-peptide affinity and is strongly influenced by nondominant anchor residues. J Exp Med 1994;180:1471–83.

29. Overwijk WW, Theoret MR, Finkelstein SE, et al. Tumor regression and autoimmunity after reversal of a functionally tolerant state of self-reactive CD8+ T cells. J Exp Med 2003;198:569–80.

30. Rechtsteiner G, Warger T, Osterloh P, Schild H, Radsak MP. Cutting edge: priming of CTL by transcutaneous peptide immunization with imiquimod. J Immunol 2005;174:2476–80.

31. Palmer DC, Chan CC, Gattinoni L, et al. Effective tumor treatment targeting a melanoma/melanocyte-associated antigen triggers severe ocular autoimmunity. Proc Natl Acad Sci U S A 2008;105:8061–6.

32. Dougherty DA. Cation-pi interactions in chemistry and biology: a new view of benzene, Phe, Tyr, and Trp. Science 1996;271:163–8.

33. Mecozzi S, West AP, Jr., Dougherty DA. Cation-pi interactions in aromatics of biological and medicinal interest: electrostatic potential surfaces as a useful qualitative guide. Proc Natl Acad Sci U S A 1996;93: 10566–71.

34. Brandl M, Weiss MS, Jabs A, Suhnel J, Hilgenfeld R. C-H. . .pi-interactions in proteins. J Mol Biol 2001; 307:357–77.

35. Steiner T, Koellner G. Hydrogen bonds with pi-acceptors in proteins: frequencies and role in stabilizing local 3D structures. J Mol Biol 2001;305:535–57.

36. Weiss MS, Jabs A, Hilgenfeld R. Peptide bonds revisited. Nat Struct Biol 1998;5:676.

37. Bhattacharyya R, Chakrabarti P. Stereospecific interactions of proline residues in protein structures and complexes. J Mol Biol 2003;331:925–40.

38. MacArthur MW, Thornton JM. Influence of proline residues on protein conformation. J Mol Biol 1991;218: 397–412.

39. Dahl AM, Beverley PC, Stauss HJ. A synthetic peptide derived from the tumor-associated protein mdm2 can stimulate autoreactive, high avidity cytotoxic T lymphocytes that recognize naturally processed protein. J Immunol 1996;157:239–46.

40. Bloom MB, Perry-Lalley D, Robbins PF, et al. Identification of tyrosinase-related protein 2 as a tumor rejection antigen for the B16 melanoma. J Exp Med 1997; 185:453–9.

41. Mennuni C, Calvaruso F, Facciabene A, et al. Efficient induction of T-cell responses to carcinoembryonic antigen by a heterologous prime-boost regimen using DNA and adenovirus vectors carrying a codon usage optimized cDNA. Int J Cancer 2005; 117:444–55.

42. Prlic M, Hernandez-Hoyos G, Bevan MJ. Duration of the initial TCR stimulus controls the magnitude but not functionality of the CD8+ T cell response. J Exp Med 2006;203:2135–43.

AACR American Association for Cancer Research

Cancer Research

The Journal of Cancer Research (1916–1930) | The American Journal of Cancer (1931–1940)

Design of Agonistic Altered Peptides for the Robust Induction of CTL Directed towards H-2D ^{b} in Complex with the Melanoma-Associated Epitope gp100

Marianne J.B. van Stipdonk, Daniel Badia-Martinez, Marjolein Sluijter, et al.

Cancer Res 2009;69:7784-7792. Published OnlineFirst September 29, 2009.